The Spectra of the Calcium I-Like Ions: Manganese VI, Iron VII, Cobalt VIII and Nickel IX

WILLOUGHBY M. CADY,[1] *Harvard University*

(Received December 9, 1932)

The spectra of four new ions have been added to the sequence of spectra isoelectronic with Ca I. A vacuum spark produced the radiation, which was analyzed in a vacuum spectrograph with a concave grating set for grazing incidence. The transitions observed were those between the ground configuration, $3d^2$, and the lowest configuration that combines with it, $3d\ 4p$. Nearly all the levels to be expected in these configurations were found, for all four spectra. Almost all the allowed transitions among the observed levels were identified, as were several intercombinations and other forbidden lines. Slater's theory for the levels (neglecting fine-structure) in a configuration gives a good fit with the observed multiplets, especially in $3d\ 4p$, which is remote from other odd configurations. In $3d^2$, $^1D_2$ is evidently perturbed by $3d\ 4s$.

THE observations here reported are an extension of those of Russell and Saunders[2] and Russell[3] on Ca I, Russell and Meggers[4] on Sc II, Russell and Lang[5] on Ti III, and White[6] on V IV and Cr V. This sequence of ions isoelectronic with Ca I is here extended so as to include the four new spectra: Mn VI, Fe VII, Co VIII and Ni IX, with a view to a comparison of the predictions of the theory of complex spectra with experimental results obtained with highly ionized atoms.

PART I. APPARATUS

The spectrograph was somewhat similar to that described by Hoag.[7] The light from a vacuum spark passed through the slit, and fell at a glancing angle of incidence upon the concave grating, whence it was diffracted and focussed on the curved photographic plate. The vacuum container was a brass tube, 93.6 cm in length by 20.4 cm in inner diameter. Therein rested a long base-plate, which carried the grating-mounting, plate-holder, and light-baffles; this base-plate was securely keyed in place, but could be removed for adjustment of the optical parts. The slit was carried by one of the two bronze castings that covered the ends of the tube.

A vacuum was produced in the spectrograph and in the glass spark-chamber by a Cenco Megavac pump, and maintained during exposures by a four-stage Leybold mercury diffusion pump (and traps cooled with solid CO_2), backed by a Cenco Hyvac pump.

The spark was excited by the discharge of a 0.33 μf capacity from a potential of 50,000 v. The discharge circuit was made as small as possible, in order to keep its inductance low, a condition which is necessary to high ionization in the source of light. A spark-gap in air, in series with the vacuum spark, was generally employed, since this seemed to improve the violence of the excitation. When it was desired to reduce the ionization, an inductance of about 0.02 mh was connected in series with the sparks.[8]

A new design for the slit was developed, which may merit description. For permanence of focus, it is essential that the position of the slit should not vary from one exposure to another. (This requirement is particularly important in grazing incidence spectrographs.) The frequent need of cleaning from the jaws the deposit of the spark necessitates a convenient way to replace the cleaned jaws accurately. This was accomplished by clipping one of the jaws (razor-blades) against

[1] National Research Fellow, at California Institute of Technology.

[2] Russell and Saunders, Astrophys. J. **61**, 38 (1925).

[3] Russell, Astrophys. J. **66**, 184 (1927).

[4] Russell and Meggers, Bur. Stand. Sci. Pap. **22**, No. 558 (1927).

[5] Russell and Lang, Astrophys. J. **66**, 13 (1927).

[6] White, Phys. Rev. **33**, 538 (1929).

[7] Hoag, Astrophys. J. **66**, 225 (1927).

[8] Gibbs, Vieweg and Gartlein, Phys. Rev. **34**, 406 (1929).

the flat vertical surface on which it rests, in such a way that its edge was tangent to two hardened steel pins, one above the other, which are set into that surface. The second jaw is shorter than the first, and is clipped in place between the pins so as to make the slit of the desired even width. The slit-width was usually about 0.02 mm.

The grating was ruled with 30,000 lines per inch on glass and etched by R. W. Wood; its radius of curvature was 197.9 cm. The glancing angle of incidence for which it was set was 6.3°, so that the dispersion at 200A was about one A/mm. Although the entire width (about 8 cm) of the grating was illuminated, ghosts were not in evidence except near the brightest lines.[9]

Schumann plates were used, as supplied by Hilger on very thin glass, 2×20 cm, which rarely broke when bent to the requisite radius of curvature of slightly less than a meter.

Part II. Procedure

With the pressure in the spark-chamber and spectrograph at about 10^{-4} mm Hg, the spark was started. The pressure thereupon rose to about 10^{-3} mm Hg, which pressure decreased slightly during the exposure, as the electrodes became outgassed. Since, therefore, the excitation does not at once come to its full violence, about the first twenty minutes were inefficient for the highest ionization; during this time, the inductance was placed in series with the spark. During the second twenty minutes, a different area of the plate was exposed, and the inductance was not in the circuit; lines that appeared with greatly increased intensity in the second exposure were thereby known to arise from highly ionized atoms[8]. One electrode was usually of aluminum, or aluminum cored with H_3BO_3, for the excitation of standard lines simultaneously with the unknown spectrum. Sometimes a third exposure was made, after a change of electrodes, of the standard spectrum only. Usually one or two seconds elapsed between sparks. The electrodes were not water cooled.

Between exposures on the same plate, a movable diaphragm, or occulter, before the plate, was lowered a fraction of an inch; the occulter was magnetically controlled from outside the spectrograph.

[9] Mack, Stehn and Edlén, J.O.S.A. **22**, 245 (1932).

The wave-lengths were determined by comparison with the spectrum of aluminum[10] and oxygen.[11] The interpolation was made quadratically on the wave-lengths among three standards, and a correction curve[12] constructed from the other neighboring standards. Neglecting ripples in the surface of the plate, the uncorrected quadratic interpolation should be, in the present case, valid to within 0.001A over a range of 30 mm.

Since the only line-group sought was that representing transitions between the $3d\ 4p$ and the $3d^2$ configurations, which are remote from each other, and compressed, the lines were, for each element, in a short section of the plate. The general position of the group for Mn VI could be predicted by extrapolation of the frequency of the same group as a function of the ionization along the Ca I-like sequence. When the Mn VI $3d^2-3d\ 4p$ lines were located, the position of those of Fe VII was predicted, and so on. The identification of the lines was facilitated by fairly accurate predictions of term separations, based on the centroid diagrams, Figs. 1 and 2.

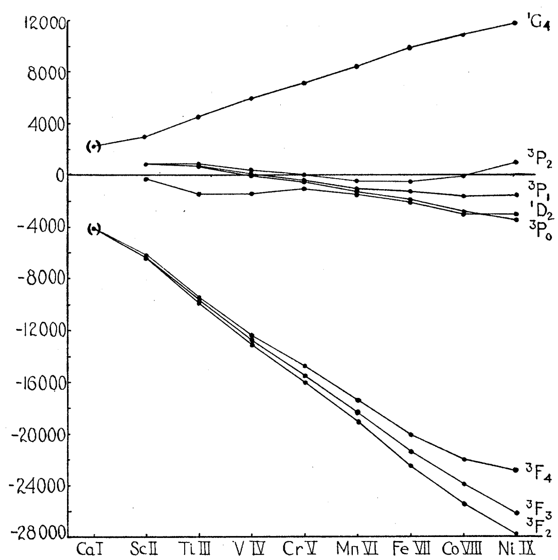

Fig. 1. Centroid diagram for $3d^2$.

[10] Söderquist and Edlén, Zeits. f. Physik **69**, 356 (1931).

[11] The writer is greatly indebted to Professor Siegbahn and to Mr. Edlén for permission to use an unpublished list of standards of oxygen, measured by Mr. Edlén at Upsala in 1931.

[12] Russell and Shenstone, J.O.S.A. **16**, 298 (1928).

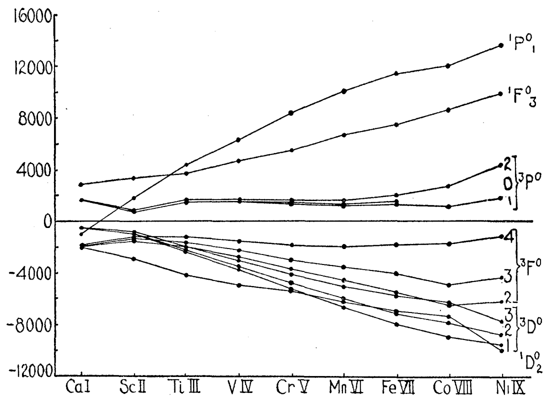

FIG. 2. Centroid diagram for $3d\ 4p$.

The plates were rich in lines; no one group could ever be said to stand out as predominant. In the plates of Mn and Fe, however, the lines of Mn VI and Fe VII, respectively, were easy to pick out before the plates were measured; in these spectra about half of the lines in the ranges measured have been identified. In the Co and Ni plates, the groups under study were much fainter, and were somewhat obscured by a preponderance of lines from lower ionization. No line was ever specifically sought during the measurement of a plate.

PART III. RESULTS

In Tables I to IV the identified lines are recorded. The symbols sometimes following the estimated intensities in the first column have the significance: n, nebulous; N, very nebulous; L, present even when the inductance is in the spark circuit, as if the line is a blend with another line

TABLE I. *Lines of Mn VI.*

Int.	λ (A)	ν (obs.)	Transition	Δν (obs.-calc.)	Int.	λ (A)	ν (obs.)	Transition	Δν (obs.-calc.)
5	307.109	325617	$^3F_3-^3F_4{}^0$	3	9	320.681	311836	$^3P_0-^3P_1{}^0$	7
3	307.842	324842	$^3F_2-^3F_3{}^0$	1	9	320.874	311649	$^3P_1-^3P_0{}^0$?	0
20	307.999	324687	$^3F_4-^3F_4{}^0$	−4	9	320.979	311547	$^3P_1-^3P_1{}^0$	−15
20	308.560	324086	$^3F_3-^3F_3{}^0$	−1	11	321.176	311356	$^3P_2-^3P_2{}^0$	−2
15	308.853	323779	$^3F_2-^3F_2{}^0$	3	9	321.541	311002	$^3P_2-^3P_1{}^0$	1
12	309.440	323164	$^3F_4-^3F_3{}^0$	0	20	325.146	307554	$^1G_4-^1F_3{}^0$?	0
10	309.579	323019	$^3F_3-^3F_2{}^0$	−3	2	326.571	306212	$^1D_2-^3F_2{}^0$	39
10	310.058	322520	$^3F_3-^3D_3{}^0$	4				$^3P_2-^3F_3{}^0$	−28
9	310.182	322391	$^3F_2-^3D_2{}^0$	0	1N	327.131	305688	$^3P_1-^3F_2{}^0$	−48
			$^3F_2-^3D_1{}^0$	−53				$^1D_2-^3D_3{}^0$	21
40	310.908	321638	$^3F_3-^3D_2{}^0$	1	2	328.129	304758	$^1D_2-^3D_2{}^0$	−30
			$^3F_4-^3D_3{}^0$	45	10	328.232	304663	$^3P_2-^3D_3{}^0$	−6
10	311.748	320772	$^1D_2-^1P_1{}^0$	−15	20	328.431	304478	$^1D_2-^1D_2{}^0$	0
8	312.692	319804	$^3P_2-^1P_1{}^0$	15	9	328.558	304360	$^3P_1-^3D_2{}^0$	9
6	314.979	317481	$^1D_2-^1F_3{}^0$?	0	5	329.043	303912	$^3P_0-^3D_1{}^0$	−6
6	320.146	312357	$^1D_2-^3P_2{}^0$	1	2	329.177	303788	$^3P_2-^3D_2{}^0$	−2
9	320.598	311917	$^3P_1-^3P_2{}^0$	−2	5	329.320	303656	$^3P_1-^3D_1{}^0$	5

TABLE II. *Lines of Fe VII.*

Int.	λ (A)	ν (obs.)	Transition	Δν (obs.-calc.)	Int.	λ (A)	ν (obs.)	Transition	Δν (obs.-calc.)
6	231.047	432813	$^3F_3-^3F_4{}^0$	−22	4	236.501	422832	$^1D_2-^1F_3{}^0$?	0
5	231.641	431702	$^3F_2-^3F_3{}^0$	0	0N	239.605	417354	$^1D_2-^3P_2{}^0$	15
8	231.715	531564	$^3F_4-^3F_4{}^0$	13	8	240.075	416537	$^3P_1-^3P_2{}^0$	18
8	232.248	430574	$^3F_3-^3F_3{}^0$	−3	7	240.105	416484	$^3P_0-^3P_1{}^0$	37
6	232.432	430233	$^3F_2-^3F_2{}^0$	−14	1	240.370	416025	$^3P_1-^3P_0{}^0$?	9
2	232.579	429962	$^3F_2-^3D_3{}^0$	−5	1n	240.451	415886	$^3P_1-^3P_1{}^0$	9
3	232.945	429286	$^3F_4-^3F_3{}^0$	−7	5	240.563	415692	$^3P_2-^3P_2{}^0$	0
10	233.021	429146	$^3F_3-^3F_2{}^0$	24	1N	240.937	415047	$^3P_2-^3P_1{}^0$	−1
2N	233.187	428840	$^3F_3-^3D_3{}^0$	−2	50	243.375	410889	$^1G_4-^1F_3{}^0$?	0
8	233.309	428617	$^3F_2-^3D_2{}^0$	29	4	244.092	409682	$^3P_2-^3F_3{}^0$	23
8	233.703	427893	$^3F_2-^3D_1{}^0$	66	7	244.524	408958	$^3P_1-^3F_2{}^0$	−75
3	233.770	427771	$^3F_3-^1D_2{}^0$	16	4	244.803	408492	$^1D_2-^1D_2{}^0$	8
3	233.940	427460	$^3F_3-^3D_2{}^0$	−3	8	245.141	407928	$^3P_2-^3D_3{}^0$	4
			$^3F_4-^3D_3{}^0$	−98	7	245.481	407364	$^3P_1-^3D_2{}^0$	−10
9	234.339	426732	$^1D_2-^1P_1{}^0$	−22	3	245.596	407173	$^3P_0-^3D_1{}^0$	−10
15B?	234.779	425932	$^3P_1-^1P_1{}^0$?	−4	10	245.926	406626	$^3P_1-^3D_1{}^0$	13
10	235.232	425112	$^3P_2-^1P_1{}^0$	5	3	245.973	406549	$^3P_2-^3D_2{}^0$	4

TABLE III. *Lines of Co VIII.*

Int.	λ (A)	ν (obs.)	Transition	Δν (obs.-calc.)
3*n*	181.994	549469	${}^3F_3-{}^3F_4^0$	92
10*Ln*	182.665	547450	${}^3F_2-{}^3F_3^0$	−178
			${}^3F_4-{}^3F_4^0$	−14
4*N*	183.125	546075	${}^3F_3-{}^3F_3^0$	−32
			${}^3F_2-{}^3F_2^0$	−27
3	183.542	544834	${}^3F_3-{}^3D_3^0$	2
			${}^3F_2-{}^3D_2^0$	41
2	183.689	544398	${}^3F_4-{}^3F_3^0$	204
4*n*	183.721	544304	${}^3F_3-{}^3F_2^0$	−277
7	183.922	543709	${}^3F_2-{}^3D_1^0$	22
3	183.941	543653	${}^3F_3-{}^1D_2^0$	−82
3*L*	184.053	543318	${}^3F_3-{}^3D_2^0$	46
70*B*	184.201	542885	${}^3F_4-{}^3D_3^0$	−34
3*LN*	184.421	542238	${}^1D_2-{}^1P_1^0$	16
6	185.432	539281	${}^3P_2-{}^1P_1^0$	−15
0	185.585	538837	${}^1D_2-{}^1F_3^0$?	0
2	187.666	532862	${}^1D_2-{}^3P_2^0$	−42

Int.	λ (A)	ν (obs.)	Transition	Δν (obs.-calc.)
2	188.154	531480	${}^3P_1-{}^3P_2^0$	−59
2	188.232	531259	${}^3P_0-{}^3P_1^0$	89
4*n*	188.673	530018	${}^3P_1-{}^3P_1^0$	17
			${}^3P_2-{}^3P_2^0$	39
4	189.249	528404	${}^3P_2-{}^3P_1^0$	−37
5	190.514	524896	${}^1G_4-{}^1F_3^0$?	0
2	190.843	523991	${}^1D_2-{}^3D_3^0$	48
1	190.954	523686	${}^1D_2-{}^3F_2^0$	−6
7*L*	191.247	522884	${}^1D_2-{}^1D_2^0$	38
3	191.465	522289	${}^3P_1-{}^3F_2^0$	−38
			${}^3P_2-{}^3F_3^0$	−4
2	191.753	521504	${}^3P_1-{}^1D_2^0$	23
10*L*	191.923	521042	${}^3P_0-{}^3D_1^0$	−39
			${}^3P_1-{}^3D_2^0$	24
			${}^3P_2-{}^3D_3^0$	24
9*L*	192.328	519945	${}^3P_1-{}^3D_1^0$	33
1	192.549	519348	${}^3P_2-{}^3D_2^0$	−110

TABLE IV. *Lines of Ni IX.*

Int.	λ (A)	ν (obs.)	Transition	Δν (obs.-calc.)
6	146.068	684613	${}^3F_3-{}^3F_4^0$	29
4	146.777	681305	${}^3F_3-{}^3F_3^0$	−101
			${}^3F_4-{}^3F_4^0$	29
			${}^3F_2-{}^3F_2^0$	78
6	147.154	679560	${}^3F_2-{}^3D_3^0$	−66
			${}^3F_3-{}^3F_2^0$	−21
0	147.370	678563	${}^3F_2-{}^3D_2^0$	−66
0	147.490	678012	${}^3F_4-{}^3F_3^0$	−86
			${}^3F_3-{}^3D_3^0$	32
			${}^3F_2-{}^3D_1^0$	153
0	147.861	676311	${}^1D_2-{}^1P_1^0$	0
3	148.215	674697	${}^3F_4-{}^3D_3^0$	25
2*N*	148.688	672549	${}^1D_2-{}^1F_3^0$?	0
1	150.247	665572	${}^3P_1-{}^3P_2^0$	29

Int.	λ (A)	ν (obs.)	Transition	Δν (obs.-calc.)
0	150.459	664633	${}^3P_0-{}^3P_1^0$	−232
20	150.844	662938	${}^3P_2-{}^3P_2^0$	−30
			${}^3P_1-{}^3P_1^0$	0
1	152.043	657709	${}^1G_4-{}^1F_3^0$?	0
7	152.316	656531	${}^1D_2-{}^3F_2^0$	29
0	152.700	654879	${}^3P_1-{}^3F_2^0$	−113
			${}^1D_2-{}^3D_3^0$	−22
2*N*	152.859	654198	${}^3P_2-{}^3F_3^0$?	−44
6	152.975	653703	${}^3P_0-{}^3D_1^0$	152
1	153.212	652690	${}^1D_2-{}^1D_2^0$	−8
1	153.296	652333	${}^3P_2-{}^3F_2^0$	−84
			${}^3P_1-{}^3D_2^0$	−61
1	153.645	650849	${}^3P_2-{}^3D_3^0$	33
12*B*?	154.174	648617	${}^3P_2-{}^1D_2^0$?	4

of lower ionization; *B*, probably a blend with another line, of high ionization. The wave-lengths are, of course, for vacuum. The identifications, in the fourth column, are written with the final state first, followed by the initial state. The last column gives the difference between the term differences (as calculated from Tables V to VIII), and the observed frequencies.

Tables V to VIII give the term values. The symbol *E* following a term value signifies that the term has not been observed, but that its value has been estimated by extrapolation of the centroid diagram.

PART IV. DISCUSSION OF RESULTS

The random experimental errors can be estimated by the deviations $\Delta\nu$, column 5, Tables I to IV; actually the average of the deviations (regardless of sign) gives too low an estimate of the random errors, but it is of some value as a basis for the estimation of the latter. Table IX shows these errors.

The systematic errors cannot greatly affect the term separations within a configuration, and will not be considered; they arise mainly from the standards, of which the accuracy is probably between 0.01A and 0.03A.

All the known terms in $3d^2$ and $3d\ 4p$ are set forth graphically in the centroid diagrams, Figs. 1 and 2. The terms are there plotted relatively to the parameter F_0 (which is the $I+F_0$ of Slater[13, 14]) for the respective configurations. This may be termed the true centroid of a configuration, since, in Slater's theory, it represents the

[13] Slater, Phys. Rev. **34**, 1293 (1929).

[14] Condon and Shortley, Phys. Rev. **37**, 1025 (1931).

TABLE V. *Terms of Mn VI.*

$3d^2$		$3d\,4p$	
$^3P_0$	17773	$^3P_0{}^0$	329689 ?
$^3P_1$	18040	$^3P_1{}^0$	329602
$^3P_2$	18601	$^3P_2{}^0$	329959
$^3F_2$	0	$^3D_1{}^0$	321691
$^3F_3$	754	$^3D_2{}^0$	322391
$^3F_4$	1677	$^3D_3{}^0$	323270
$^1S_0$		$^3F_2{}^0$	323776
$^1D_2$	17603	$^3F_3{}^0$	324841
$^1G_4$	27530 ?	$^3F_4{}^0$	326368
		$^1P_1{}^0$	338390
		$^1D_2{}^0$	322081
		$^1F_3{}^0$	335084 ?

TABLE VI. *Terms of Fe VII.*

$3d^2$		$3d\,4p$	
$^3P_0$	20644	$^3P_0{}^0$	437230 ?
$^3P_1$	21214	$^3P_1{}^0$	437091
$^3P_2$	22043	$^3P_2{}^0$	437735
$^3F_2$	0	$^3D_1{}^0$	427827
$^3F_3$	1125	$^3D_2{}^0$	428588
$^3F_4$	2409	$^3D_3{}^0$	429967
$^1S_0$		$^3F_2{}^0$	430247
$^1D_2$	20396	$^3F_3{}^0$	431702
$^1G_4$	32339 ?	$^3F_4{}^0$	433960
		$^1P_1{}^0$	447150
		$^1D_2{}^0$	428880
		$^1F_3{}^0$	443228 ?

TABLE VII. *Terms of Co VIII.*

$3d^2$		$3d\,4p$	
$^3P_0$	22606	$^3P_0{}^0$	554076 *E*
$^3P_1$	23775	$^3P_1{}^0$	553776
$^3P_2$	25335	$^3P_2{}^0$	555314
$^3F_2$	0	$^3D_1{}^0$	543687
$^3F_3$	1521	$^3D_2{}^0$	544793
$^3F_4$	3434	$^3D_3{}^0$	546353
$^1S_0$		$^3F_2{}^0$	546102
$^1D_2$	22410	$^3F_3{}^0$	547628
$^1G_4$	36351 ?	$^3F_4{}^0$	550898
		$^1P_1{}^0$	564632
		$^1D_2{}^0$	545256
		$^1F_3{}^0$	561247 ?

TABLE VIII. *Terms of Ni IX.*

$3d^2$		$3d\,4p$	
$^3P_0$	24308	$^3P_0{}^0$	689573 *E*
$^3P_1$	26235	$^3P_1{}^0$	689173
$^3P_2$	28810	$^3P_2{}^0$	691778
$^3F_2$	0	$^3D_1{}^0$	677859
$^3F_3$	1646	$^3D_2{}^0$	678629
$^3F_4$	4954	$^3D_3{}^0$	679626
$^1S_0$		$^3F_2{}^0$	681227
$^1D_2$	24725	$^3F_3{}^0$	683052
$^1G_4$	39565 ?	$^3F_4{}^0$	686230
		$^1P_1{}^0$	701036
		$^1D_2{}^0$	677423
		$^1F_3{}^0$	697274 ?

levels whence the several multiplets grow out. This definition of the centroid is particularly useful when a level is missing or strongly perturbed by another configuration.

The only theory of complex spectra which will be compared with the observed term schemes is that of Slater[13], which contemplates the inter-multiplet separations within a configuration, neglecting the effect of fine-structure and of perturbations between configurations. Condon and Shortley[14] have applied this theory to several cases where the observations were sufficiently complete; the data presented here provide eight new configurations in which to test the theory.

Slater's theory predicts that in a d^2 configuration which is remote from other even configurations, and in which the fine-structure separations are much less than the distances between multiplets, the frequencies of the multiplets are given by

$$^1S=F_0+14F_2+126F_4 \qquad {}^3F=F_0-8F_2-9F_4$$

$$^3P=F_0+\ 7F_2-\ 84F_4 \qquad {}^1G=F_0+4F_2+\ F_4$$

$$^1D=F_0-\ 3F_2+\ 36F_4$$

where the F's are, effectively, parameters to be adjusted to fit the data. Further, another set of parameters, F_0, F_2, G_1 and G_3, should exist, such that, in a configuration $d\cdot p$, subject to the restrictions that the multiplets are narrow and that no other odd configurations are near,

$$^1P^0=F_0+7F_2+\ \ G_1+63G_3$$

$$^3P^0=F_0+7F_2-\ \ G_1-63G_3$$

$$^1D^0=F_0-7F_2-\ 3G_1+21G_3$$

$$^3D^0=F_0-7F_2+\ 3G_1-21G_3{}^0$$

$$^1F^0=F_0+2F_2+\ 6G_1+3G_3$$

$$^3F^0=F_0+2F_2-\ 6G_1-3G_3.$$

By way of definition, the observed frequency of a multiplet is taken as the average of its fine-structure components, weighted according to their values of $2J+1$. This frequency may be called the centroid of a multiplet; it represents the position from which the fine-structure terms spread out.[15] As is to be expected, the above

[15] See, for instance, Houston, Phys. Rev. 33, 297 (1929).

TABLE IX.

	Mn VI	Fe VII	Co VIII	Ni IX
Ave. $\|\Delta\nu\|$ (cm^{-1})	11	16	47	55
Ave. $\|\Delta\lambda\|$ (A)	0.011	0.009	0.017	0.013

definition allows a somewhat better fit of the above formulas than does an unweighted mean of the terms for each multiplet.

In $3d^2$, ^1S is not known,[14] and ^1D is (except in Sc II) depressed by $3d\ 4s\ ^1D$, ^3D, of the same parity, which lies above it. Therefore we calculate the F's for $3d^2$ from the three other levels: ^3P, ^3F, and ^1G. With the parameters so determined, we compute ^1D, and compare the observed value with the one so computed. The result is in the sense of an observed depression of ^1D, except in the case of Sc II, where $3d\ 4s$ lies below $3d^2$. The possibility of a perturbation between $3d^2$, $^3P_2$ and $^1D_2$ is here neglected.

Table X shows the values of the F's for $3d^2$, and also the perturbation $p={}^1D_{\text{obs.}}-{}^1D_{\text{calc.}}$. For reference, there is also tabulated the frequency difference $f=$(centroid of $3d\ 4s$)$-$(centroid of $3d^2$), and p/Z_0, where Z_0 is the Roman numeral of the spectrum. The figures in parentheses are estimated by extrapolating from known data.[4, 5, 6]

TABLE X.

	Sc II	Ti III	V IV	Cr V	Mn VI	Fe VII	Co VIII	Ni IX
F_0	11263	9874	13141	16056	19098	22521	25438	27836
F_2	736.8	1110.4	1456	1758	2062	2402	2670	2871
F_4	51.11	83.16	119.0	148.8	181.1	211.0	233.5	243.9
p	52	−1065	−1397	−1219	−1827	−2516	−3424	−3277
f	−9939	30116	85583	154242	(250000)	(360000)	(490000)	(630000)
p/Z_0	26	−355	−349	−244	−304	−359	−428	−364

TABLE XI.

	Ca I	Sc II	Ti III	V IV	Cr V	Mn VI	Fe VII	Co VIII	Ni IX
F_0	37698	28966	79404	149903	233226	328317	435718	552606	687369
F_2	78	242	444	583	709	841	955	1032	1276
G_1	366	380	435	534	616	730	796	902	1002
G_3	−24.0	2.7	15.2	30.2	47.4	60.1	69.0	71.5	70.8
Δ^1P^0	−366	−394	−109	−165	−167	−330	−396	−604	−727
Δ^3P^0	−52	−323	−133	−43	143	122	204	240	−174
Δ^1D^0	286	−108	−113	120	435	579	786	1078	505
Δ^3D^0	−524	−290	−28	−228	−445	−697	−893	−1286	−1016
Δ^1F^0	560	607	169	254	258	525	617	951	1129
Δ^3F^0	101	505	210	70	−227	−197	−322	−378	283
Acc.	6.7%	5.9%	1.5%	1.3%	2.0%	2.5%	2.9%	3.9%	2.7%

It is to be noted that p/Z_0 is roughly constant, except for Sc II.

Table XI gives the best (least square) values of the F's and G's for $3d\ 4p$, and the discrepancy (observed − calculated) for each multiplet. As before, F_0 is tabulated relatively to the ground state, for each spectrum. The last row gives the average discrepancy (regardless of the sign of the individual discrepancies), divided by the over-all width of the configuration. The theory is not, however, quite as successful as is indicated by this measure of its accuracy; the parameters could be adjusted to fit any six arbitrarily chosen numbers, with an "accuracy" of better than 50 percent.

The observed departures from theory in $3d\ 4p$ probably arise mainly from magnetic perturbations (between terms of like J), which were not contemplated by Slater. The predictions of Johnson[16] could be tested here, but this has not been undertaken.

The unobserved configuration $4s\ 4p$ is about as close to $3d\ 4p$ as $3d\ 4s$ is to $3d^2$, since the difference is, in both cases, that between a $3d$ and a $4s$ electron. Perhaps, then, the inaccuracy of the theory in $3d\ 4p$ is partly to be referred to a perturbation by $4s\ 4p$, $^1P^0$ and $^3P^0$. The apparent absence of any large perturbation of this sort can

[16] Johnson, Phys. Rev. **38**, 1628 (1931).

perhaps be construed as evidence against the correctness of the above discussion of $3d^2$.

In the centroid diagram for $3d\ 4p$, Fig. 2, we observe that $^3D^0$ and $^3F^0$ lie very close together. This results in a confusion of identity between $^3D_2{}^0$ and $^3F_2{}^0$, and between $^3D_3{}^0$ and $^3F_3{}^0$; forbidden lines $^3P-{}^3F^0$ appear, since ^3P combines with $^3D^0$. The L-values of the four mixed levels might have been assigned oppositely, with equal justification. Many intercombination lines appear between the singlet and triplet systems, further evidence that we are dealing with coupling that is not strictly LS. The partial inversion of $^3P^0$ probably arises from a perturbation between $^1P_1{}^0$ and $^3P_1{}^0$, in the sense of a depression of the latter to a point below $^3P_0{}^0$; in Ca I, however, $^3P^0$ is normal, because $^1P^0$ is here below $^3P^0$.

It is with great pleasure that I acknowledge my debt to Professor Lyman of Harvard University, under whose guidance all the experimental part of this research was done, and to Professor Houston of the California Institute of Technology, for his valuable suggestions as to the preparation of Part IV.